THE AMERICAN MINERALOGIST, VOL. 56, MARCH-APRIL, 1971

THE CRYSTAL STRUCTURE OF AENIGMATITE

E. CANNILLO AND F. MAZZI, *Centro di studio del C.N.R. per la cristallografia strutturale, Istituto di Mineralogia dell' Università di Pavia, Italy.*

AND

J. H. FANG, PAUL D. ROBINSON, AND Y. OHYA, *Department of Geology, Southern Illinois University, Carbondale, Illinois, U.S.A.*

ABSTRACT

Aenigmatite, $Na_2Fe_5TiSi_6O_{20}$, is triclinic $P\bar{1}$, with $a=10.406(13)$, $b=10.813(14)$, $c=8.926(6)$ Å, $\alpha=104°\ 56'(9)$, $\beta=96°52'(11)$, $\gamma=125°19'(6)$, and $Z=2$. The structure was solved, independently and simultaneously, by Patterson syntheses and by the symbolic addition procedure. Three-dimensional refinement with 921 "observed" reflections (photographic data) from a Naujakasik, Greenland, crystal gave $R_{hkl}=0.075$ and with 1501 "observed" reflections (counter data) from a Kola, Greenland crystal gave $R_{hkl}=0.072$.

A distinct pseudo-monoclinic symmetry, based on a cell with parameters: $a_m=12.120$, $b_m=2\times14.815$, $c_m=10.406$ Å, $\alpha_m=90°4'$, $\beta_m=127°9'$, $\gamma_m=89°44'$ (matrix of transformation $[011/\bar{1}\bar{2}2/100]$), $Z=8$, emphasizes the similarity of its crystal structure with that of sapphirine $[(Mg, Al)_8O_2(Si, Al)_6O_{18}$, $a=11.266$, $b=14.401$, $c=9.929$ Å, $\beta=125\ °46'$, $Z=4$, space group $P2_1/a]$.

The crystal structure consists of two sets of polyhedral layers parallel to the pseudo-monoclinic (100) plane which alternate along the x^*-direction. The first layer is formed by Fe-octahedra, Ti-octahedra and distorted Na-square antiprisms and the second by $[Si_6O_{18}]_\infty$ chains connected by Fe-octahedra. The silicate chains are of the type found in sapphirine, *i.e.* pyroxene-like chains where, in the repeat distance of four tetrahedra, two consecutive tetrahedra share a common vertex with two additional tetrahedra.

The formation of twins frequently found in volcanic aenigmatite is interpreted as due to the "frozen" effect of crystallization under rapid, inequilibrium conditions prevailing during the crystal growth.

INTRODUCTION

Aenigmatite was discovered by Breithaupt in 1865 (Kelsey and McKie, 1964). It is not clear why it was named aenigmatite, but it could not be more appropriate for the mineral has been a crystallochemical enigma since its discovery. A comprehensive and complete study of aenigmatite by Kelsey and McKie in 1964 did much to clear up the confusion and conflicts hitherto reported in the literature. They established and characterized the mineral as having an idealized unit cell content of $Na_4Fe_{10}^{2+}Ti_2Si_{12}O_{40}$ with the cell parameters quoted in the abstract. Furthermore, they predicted that the crystal structure of aenigmatite contains pyroxene-like chains running parallel to the *a*-axis. However, the structure remained unsolved for years until recently when it was independently and simultaneously solved by three groups of crystallographic mineralogists: by Merlino (1970a) by Cannillo and Mazzi, and by Fang, Robinson, and Ohya.

This paper presents the results of the last two groups. It should be mentioned that a manuscript was submitted to this journal by Cannillo and Mazzi (*CM*) on August 7, 1970. Subsequently, after discussions with the Editor and correspondence between the two groups, it was decided that a joint paper would produce a more complete publication on this mineral structure. The contributions added by the American group (*FRO*) are explicitly indicated.

Experimental

(*CM*) A small sphere ($r=0.017$ cm) was ground from a fragment of an aenigmatite crystal from Naujakasik, Greenland. Precession photographs of the $0kl$, $1kl$, $2kl$, $3kl$ and $hk0$ levels were taken with exposures at fixed time employing MoKα radiation. A total of 1617 independent reflections was inspected; 921 of them were measured with a microdensitometer. The remaining data were too faint to be satisfactorily measured or did not noticeably blacken the films. The usual corrections, including that for absorption ($\mu r=1.06$), were applied.

This sample of aenigmatite appears to be moderately twinned: we estimated a ratio of roughly 10:1 between the sizes of the twin individuals from the intensities of symmetrical spots, which appear separated on photographs of odd-h-levels. Unfortunately the symmetrical reflections due to the twinning are superimposed on even-h-level photographs. No correction was applied because of the small contribution by one of the twin individuals and because the structure amplitudes of superimposed reflections would have a fairly similar value, as a consequence of the peculiar crystal structure of aenigmatite.

(*FRO*) Data were collected from a small, six-faced crystal of volume 0.136×10^{-2}mm^3. The integrated intensities were measured with a Supper-Pace automatic single-crystal diffractometer with CuKα radiation. The intensities of 2582 reflections from the zeroth to ninth layer around the c axis were measured. The data were corrected for Lp and absorption ($\mu r=2.46$) with the ACAC program of C. T. Prewitt (unpublished). After data reduction to obtain $|F(\text{obs})|$, 1518 reflections were considered to be non-zero.

Structure Determination

(*CM*) The crystal lattice shows a distinct monoclinic pseudosymmetry, since the $[12\bar{2}]$ row is nearly perpendicular to the $(01\bar{1})$ plane, *i.e.* $[12\bar{2}]\wedge(01\bar{1})=89°44'$. Thus, the determination was initiated by considering a "monoclinic" unit-cell having a volume four times that of the triclinic cell, with parameters: $a_m=12.120$, $b_m=2\times14.815$, $c_m=10.406$ Å,

$\alpha_m = 90°4'$, $\beta_m = 127°9'$, $\gamma_m = 89°44'$ and $Z = 8$. Such a cell is A-centered with two further lattice points at $(\frac{1}{2}, \frac{1}{4}, \frac{1}{4})$ and $(\frac{1}{2}, \frac{3}{4}, \frac{3}{4})$. The transformation matrix from the Kelsey-McKie triclinic cell to the above "monoclinic" cell is $[011/\bar{1}\bar{2}2/100]$.

The reflections obtained from $0kl$ and $2kl$ photographs ($hk0_m$ and $hk2_m$ for the above pseudo-monoclinic unit-cell) were first considered. A simple visual observation of the spot intensities shows a symmetry practically monoclinic, which leads to the identification of a subcell having $b_m' = b_m/2$ and $c_m' = c_m/2$, consistent with the space group $I2/c$. This observation suggested that most of the cations in the monoclinic pseudo-cell should repeat with periods $b_m/2$ and $c_m/2$; the remaining ones should lie in positions consistent with the space group $I2/c$: however half of the latter atomic positions are vacant, contributing to the real repeat distance of b_m and c_m. The $hk0_m$-Patterson projection, an $hk2_m$-generalized Patterson projection, as well as a three dimensional Patterson synthesis allowed the conclusion that nearly all (Fe, Ti, Na) should lie on the "two-fold axes" of the sub-cell, with the remaining atoms in general positions. The pyroxene-chain suggested by Kelsey and McKie was confirmed; however, it should be formed by only $\frac{2}{3}$ of the silicon atoms in the unit cell, and each $[SiO_4]$ tetrahedron should be repeated with translations $b_m/2$ and $c_m/2$. On the other hand, each tetrahedron formed by the remaining $\frac{1}{3}$ of the silicon atoms should be connected by a vertex to a tetrahedron of the chains, and such tetrahedra should have the actual repeat distance b_m and c_m. This arrangement of tetrahedra bears similarity to that of sapphirine. The latter mineral, $(Mg, Al)_8 \cdot (Si, Al)_6O_{20}$, has a formula unit comparable to that of aenigmatite and its cell parameters, $a = 11.266$, $b = 14.401$, $c = 9.926$ Å, $\beta = 125°46'$, $Z = 4$ and $P2_1/a$ (Moore, 1969), are also similar to those of aenigmatite described with the monoclinic pseudo-cell.

The trial positional parameters were thus determined both from the Patterson syntheses and analogy with the crystal structure of sapphirine.

(*FRO*) The structure was solved by the symbolic addition procedure. However, because of the high degree of subperiodicity of most atoms within the triclinic unit cell, the determination was not straightforward. Initially, signs and symbols were manually determined for the 20 reflections with the highest values of normalized structure factors. The phase determination was then extended to reflections with $|E| > 1.5$ with the aid of the SORTE program of Bednowitz (1970). The three best E maps were examined and it was found that, although the octahedral walls were revealed in all three maps, no silicon tetrahedral chains were discernible. In spite of much labor and computation some silicon and

oxygen atoms could not be extracted from any of the above E maps. We then re-examined the distribution of the intensities and realized that there existed a triclinic pseudo-cell with $a/2$, b, c of the original triclinic cell. Normalized structure factors were then recalculated for the pseudo-cell, and the symbolic addition procedure was again manually initiated. The E maps thus obtained enabled us to fix the orientation and location of the octahedral walls, and also, to find some indications of the silicon positions. Returning to the full triclinic cell and using the sign information derived from the pseudo-cell, we determined more new signs. However, signs of a large number of reflections with $E>1.0$ remained undetermined, since we were now only accepting new signs with probabilities of .999 and at least four confirming interactions. At this point there were 10 undetermined reflections with E values greater than 2.0. By manual manipulation of these reflections it was found that 8 of the 10 could be related by the addition of 3 new symbols. The symbolic addition procedure was then continued with the addition of the three new symbols and all 607 reflections above $E=1.0$ were determined in terms of signs and symbols. By referring back to the pseudo-cell it was possible to determine the actual signs of the 3 new symbols. The resulting E-map clearly revealed every atom of the structure with proper peak heights. A structure factor calculation performed at this point yielded an R-index of 0.273.

It is interesting to note the following: (1) despite the extremely high degree of pseudo-symmetry, the Σ_2 relationship could still be made to work perfectly. However, without frequent manual intervention, it would have failed, (2) there was a preponderance of positive phases for reflections with $E>1.5$, and (3) there were parallels between the difficulties in the phase determination of aenigmatite and those that were encountered by Moore in his solution of the sapphirine structure.

Refinement

(*CM*) Trial parameters were refined through several least-squares cycles, by using a local version of the Busing, Martin and Levy ORFLS program [no weighting scheme; form factors for neutral atoms obtained from Hanson, Herman, Lea and Skillman (1964)]. Because of the limited number of experimental data, only isotropic temperature factors were used in the refinement. The idealized chemical composition of Kelsey and McKie was assumed; the uniform values of the thermal vibration obtained for the same kind of atoms are consistent with this assumption. The R index is 0.075 for all 921 measured reflections. The

TABLE 1. FINAL ATOMIC COORDINATES AND ISOTROPIC TEMPERATURE FACTORS FOR AENIGMATITE[a]

Atom		x		y		z		B(Å²)	
CM	*FRO*	*CM*	*FRO*	*CM*	*FRO*	*CM*	*FRO*	*CM*	*FRO*
Fe(1)	*M*(1)	0	0	0	0	½	½	0.89 (7)	0.76 (7)[b]
Fe(2)	*M*(2)	0	0	½	½	0	0	0.85 (7)	0.73 (7)[b]
Fe(3)	*M*(3)	.3193 (6)	.3214 (3)	.8513 (4)	.8528 (3)	.1779 (4)	.1779 (3)	0.91 (5)	0.92 (5)[b]
Fe(4)	*M*(4)	.7670 (6)	.7655 (3)	.8203 (3)	.8199 (3)	.1517 (4)	.1511 (3)	0.68 (5)	0.93 (5)[b]
Fe(5)	*M*(5)	.0952 (7)	.0961 (4)	.9382 (4)	.9392 (3)	.0522 (4)	.0530 (3)	0.98 (5)	1.01 (5)[b]
Fe(6)	*M*(6)	.5962 (7)	.5959 (3)	.9435 (4)	.9432 (3)	.0662 (4)	.0661 (3)	0.82 (5)	0.92 (5)[b]
Ti	*M*(7)	.9970 (9)	.9970 (4)	.7428 (4)	.7434 (4)	.2565 (5)	.2577 (3)	0.62 (6)	0.70 (5)[b]
Na(1)	Na(1)	.2092 (17)	.2089 (8)	.6289 (10)	.6298 (8)	.3893 (10)	.3893 (7)	1.33 (16)	0.55 (11)[b]
Na(2)	Na(2)	.6627 (16)	.6607 (8)	.6127 (10)	.6117 (9)	.3733 (10)	.3741 (8)	1.42 (16)	1.06 (13)[b]
Si(1)	*T*(1)	.4798 (12)	.4768 (5)	.2333 (6)	.2345 (5)	.3311 (7)	.3313 (5)	0.82 (9)	0.41 (8)[b]
Si(2)	*T*(2)	.9879 (13)	.9864 (5)	.2363 (6)	.2363 (5)	.3456 (7)	.3466 (5)	0.68 (9)	0.39 (7)[b]
Si(3)	*T*(3)	.7925 (12)	.7921 (5)	.3435 (7)	.3435 (5)	.2424 (7)	.2416 (4)	0.84 (9)	0.40 (7)[b]
Si(4)	*T*(4)	.2782 (11)	.2772 (5)	.3364 (6)	.3382 (5)	.2257 (7)	.2252 (5)	0.86 (10)	0.62 (8)[b]
Si(5)	*T*(5)	.6478 (13)	.6487 (5)	.9448 (7)	.9448 (5)	.4450 (7)	.4447 (5)	0.76 (9)	0.50 (8)[b]
Si(6)	*T*(6)	.3525 (11)	.3528 (5)	.5573 (6)	.5588 (5)	.0501 (7)	.0501 (5)	0.78 (9)	0.51 (8)[b]
O(1)	O(1)	.3600 (31)	.3542 (14)	.0684 (17)	.0641 (14)	.1630 (17)	.1621 (13)	1.02 (24)	0.64 (21)
O(2)	O(2)	.8640 (29)	.8611 (14)	.0688 (18)	.0666 (13)	.1800 (18)	.1807 (12)	1.41 (29)	0.43 (20)
O(3)	O(3)	.5488 (29)	.5540 (15)	.9535 (17)	.9534 (15)	.2957 (18)	.2958 (13)	1.20 (27)	0.75 (21)
O(4)	O(4)	.0087 (28)	.0151 (15)	.9233 (17)	.9258 (15)	.2648 (17)	.2670 (13)	1.19 (25)	0.83 (21)
O(5)	O(5)	.2364 (28)	.2353 (15)	.8751 (17)	.8747 (14)	.3951 (18)	.3933 (13)	1.19 (27)	0.65 (20)
O(6)	O(6)	.7523 (28)	.7541 (15)	.8821 (17)	.8843 (14)	.3912 (18)	.3902 (13)	1.10 (26)	0.63 (21)
O(7)	O(7)	.4967 (27)	.4929 (15)	.1947 (17)	.1948 (15)	.4965 (17)	.4973 (13)	1.00 (25)	0.75 (22)
O(8)	O(8)	.9603 (28)	.9575 (14)	.7756 (16)	.7755 (14)	.4843 (17)	.4871 (12)	0.98 (25)	0.58 (20)
O(9)	O(9)	.9069 (28)	.8996 (15)	.3300 (18)	.3230 (14)	.3717 (18)	.3735 (13)	1.44 (28)	0.76 (20)
O(10)	O(10)	.4091 (25)	.4034 (15)	.3408 (15)	.3364 (15)	.3539 (16)	.3529 (13)	0.75 (22)	0.93 (22)
O(11)	O(11)	.6710 (29)	.6653 (14)	.1773 (18)	.1744 (14)	.0749 (18)	.0709 (12)	1.44 (29)	0.57 (20)
O(12)	O(12)	.1565 (27)	.1570 (14)	.1694 (16)	.1688 (14)	.0646 (17)	.0612 (12)	1.02 (26)	0.57 (20)
O(13)	O(13)	.5197 (27)	.5233 (15)	.7094 (17)	.7108 (14)	.0365 (17)	.0393 (12)	1.04 (25)	0.56 (20)
O(14)	O(14)	.0671 (27)	.0673 (13)	.7334 (16)	.7340 (13)	.0776 (16)	.0757 (12)	0.78 (23)	0.37 (19)
O(15)	O(15)	.2453 (32)	.2417 (15)	.6098 (18)	.6060 (16)	.1152 (19)	.1120 (13)	1.51 (30)	0.89 (23)
O(16)	O(16)	.7572 (29)	.7510 (14)	.6022 (18)	.6018 (15)	.1230 (18)	.1275 (13)	1.39 (29)	0.64 (21)
O(17)	O(17)	.4040 (27)	.4002 (14)	.4995 (16)	.5015 (14)	.1882 (17)	.1883 (12)	1.01 (24)	0.52 (20)
O(18)	O(18)	.9370 (27)	.9363 (16)	.5164 (17)	.5147 (16)	.2269 (17)	.2264 (14)	1.15 (26)	1.09 (23)
O(19)	O(19)	.1708 (26)	.1648 (14)	.3661 (16)	.3649 (14)	.3271 (16)	.3183 (12)	0.91 (24)	0.62 (20)
O(20)	O(20)	.6749 (26)	.6731 (15)	.3640 (16)	.3626 (15)	.3422 (16)	.3366 (13)	0.93 (24)	0.99 (21)

[a] Standard errors in parentheses. [b] Anisotropic temperature factors converted to equivalent isotropic.

observed and calculated structure factors are on deposit.[1] The atomic parameters are listed in Table 1; bond distances and tetrahedral angles are in Tables 2 and 3.

(*FRO*) A least-squares refinement of the positional parameters obtained from the *E* map was performed. After three cycles of Finger's RFINE program (1969), with isotropic temperature factors, the *R* index for the 1518 non-zero data was 9.2 percent. The coefficients for the analytical form factors of ionized atoms were obtained from Cromer and Mann (1968). The weights were calculated from the variance for each structure factor,

$$\sigma^2 = F^2/4(T-B)\,[T + B + 0.0009\,(T-B)^2]$$

where T = total count, B = average background count, and the additional term involving $(T-B)$ is to allow for errors proportional to the net count, such as variation in the beam intensity and absorption errors. At this

[1] To obtain a copy, order NAPS Document No. 01314 from National Auxiliary Publications Service of A.S.I.S., c/o CCM Information Corporation, 909 Third Avenue, New York, New York 10022; remitting $4.00 for microfiche or $5.60 for photocopies, in advance, payable to CCMIC-NAPS.

TABLE 2. INTERATOMIC DISTANCES (Å) IN AENIGMATITE[a]

Tetrahedral coordination around *T* sites					
	CM	*FRO*		*CM*	*FRO*
T (1)–O(1)	1.61 (2)	1.640 (11)	*T* (2)–O (8)	1.61 (2)	1.593 (11)
–O (10)	1.68 (2)	1.653 (14)	–O (2)	1.61 (2)	1.622 (11)
–O (7)	1.65 (2)	1.662 (10)	–O (9)	1.64 (3)	1.633 (13)
–O (20)	1.64 (2)	1.663 (13)	–O (19)	1.65 (2)	1.659 (11)
Mean	1.64	1.654	Mean	1.63	1.627
T (3)–O (18)	1.64 (2)	1.632 (12)	*T* (4)–O (12)	1.59 (2)	1.611 (11)
–O (11)	1.61 (2)	1.643 (11)	–O (19)	1.64 (2)	1.626 (12)
–O (20)	1.68 (3)	1.659 (13)	–O (17)	1.64 (2)	1.628 (11)
–O (9)	1.65 (2)	1.670 (12)	–O (10)	1.64 (2)	1.645 (12)
Mean	1.64	1.651	Mean	1.63	1.628
T (5)–O (3)	1.64 (2)	1.613 (12)	*T* (6)–O (15)	1.62 (3)	1.610 (14)
–O (6)	1.64 (3)	1.632 (13)	–O (13)	1.61 (2)	1.615 (11)
–O (7)	1.67 (2)	1.652 (11)	–O (16)	1.61 (2)	1.643 (12)
–O (5)	1.65 (2)	1.662 (12)	–O (17)	1.68 (2)	1.658 (11)
Mean	1.65	1.640	Mean	1.63	1.632

TABLE 2. INTERATOMIC DISTANCES (Å) IN AENIGMATITE[a]

Octahedral coordination around *M* sites

	CM	*FRO*		*CM*	*FRO*
M (1)–O (6)	2.04 (2)	2.035 (12)	*M* (2)–O (15)	2.05 (3)	2.029 (12)
–O (4)	2.08 (2)	2.087 (11)	–O (14)	2.07 (2)	2.075 (11)
–O (8)	2.17 (2)	2.169 (12)	–O (18)	2.20 (2)	2.196 (11)
Mean	2.10	2.097	Mean	2.11	2.100
M (3)–O (3)	1.94 (2)	1.976 (13)	*M* (4)–O (13)	2.07 (2)	2.023 (12)
–O (14)	2.07 (2)	2.090 (11)	–O (4)	2.04 (3)	2.106 (13)
–O (1)	2.18 (2)	2.153 (12)	–O (6)	2.12 (2)	2.108 (11)
–O (15)	2.13 (2)	2.161 (14)	–O (12)	2.18 (2)	2.151 (10)
–O (11)	2.22 (2)	2.196 (10)	–O (2)	2.18 (2)	2.163 (11)
–O (5)	2.23 (2)	2.231 (11)	–O (16)	2.25 (2)	2.226 (13)
Mean	2.13	2.134	Mean	2.14	2.130
M (5)–O (1)	2.17 (3)	2.119 (12)	*M* (6)–O (13)	2.09 (2)	2.097 (12)
–O (12)	2.12 (2)	2.128 (12)	–O (3)	2.15 (2)	2.135 (11)
–O (14)	2.14 (2)	2.129 (11)	–O (11)′	2.15 (2)	2.150 (12)
–O (12)′	2.16 (2)	2.155 (12)	–O (1)	2.14 (2)	2.155 (10)
–O (2)	2.16 (2)	2.177 (10)	–O (2)	2.21 (3)	2.193 (11)
–O (4)	2.20 (2)	2.184 (11)	–O (11)	2.27 (2)	2.215 (12)
Mean	2.16	2.149	Mean	2.17	2.158

M (7)–O (4)	1.86 (2)	1.848 (13)
–O (14)	1.84 (2)	1.863 (10)
–O (5)	2.00 (2)	1.989 (12)
–O (16)	1.98 (2)	2.021 (12)
–O (18)	2.08 (2)	2.095 (14)
–O (8)	2.09 (2)	2.117 (11)
Mean	1.98	1.989

Coordination around Na

	CM	*FRO*		*CM*	*FRO*
Na (1)–O (7)	2.35 (3)	2.388 (13)	Na (2)–O (17)	2.36 (2)	2.385 (13)
–O (18)	2.39 (3)	2.390 (14)	–O (8)	2.39 (3)	2.388 (13)
–O (5)	2.49 (2)	2.489 (14)	–O (6)	2.44 (2)	2.467 (14)
–O (15)	2.49 (2)	2.506 (12)	–O (16)	2.55 (2)	2.495 (12)
–O (19)	2.52 (2)	2.509 (13)	–O (10)	2.51 (2)	2.538 (13)
–O (20)	2.51 (2)	2.562 (12)	–O (10)′	2.64 (2)	2.611 (13)
–O (9)	2.64 (2)	2.589 (12)	–O (20)	2.71 (2)	2.709 (15)
–O (9)′	2.87 (2)	2.948 (13)	–O (19)	2.88 (2)	2.969 (12)
Mean	2.53	2.548	Mean	2.56	2.570

[a] Cation designators are those of the *FRO* group. Standard errors in parentheses.

TABLE 3. TETRAHEDRAL BOND ANGLES IN AENIGMATITE[a]

	CM	*FRO*		*CM*	*FRO*
O(1)–*T*(1)–O(7)	113.1 (8)	111.7 (.6)	O(10)–*T*(4)–O(12)	113.6 (1.0)	111.4 (.6)
O(1)–*T*(1)–O(10)	110.3 (1.3)	110.2 (.6)	O(10)–*T*(4)–O(17)	102.5 (1.0)	105.1 (.6)
O(1)–*T*(1)–O(20)	115.0 (1.2)	113.6 (.6)	O(10)–*T*(4)–O(19)	107.2 (9)	109.2 (.6)
O(7)–*T*(1)–O(10)	109.0 (1.0)	108.7 (.6)	O(12)–*T*(4)–O(17)	113.4 (8)	113.3 (.6)
O(7)–*T*(1)–O(20)	103.4 (1.0)	104.6 (.6)	O(12)–*T*(4)–O(19)	110.6 (1.2)	109.9 (.6)
O(10)–*T*(1)–O(20)	105.5 (9)	107.8 (.6)	O(17)–*T*(4)–O(19)	109.0 (1.0)	107.8 (.6)
Mean	109.4	109.4	Mean	109.4	109.4
O(2)–*T*(2)–O(8)	118.7 (8)	118.0 (.6)	O(3)–T(5)–O(5)	108.6 (1.0)	109.3 (.6)
O(2)–*T*(2)–O(9)	108.5 (1.3)	107.6 (.6)	O(3)–*T*(5)–O(6)	114.5 (1.1)	112.9 (.6)
O(2)–*T*(2)–O(19)	110.8 (1.1)	109.1 (.6)	O(3)–*T*(5)–O(7)	107.2 (1.2)	108.8 (.6)
O(8)–*T*(2)–O(9)	108.9 (1.1)	109.8 (.6)	O(5)–*T*(5)–O(6)	113.4 (1.3)	113.2 (.6)
O(8)–*T*(2)–O(19)	102.8 (1.0)	104.3 (.6)	O(5)–*T*(5)–O(7)	106.6 (9)	106.5 (.6)
O(9)–*T*(2)–O(19)	106.3 (1.0)	107.6 (.6)	O(6)–*T*(5)–O(7)	106.0 (1.0)	105.9 (.6)
Mean	109.3	109.4	Mean	109.4	109.4
O(9)–*T*(3)–O(11)	111.4 (1.0)	111.3 (.6)	O(13)–*T*(6)–O(15)	111.4 (1.0)	113.6 (.6)
O(9)–*T*(3)–O(18)	101.7 (1.1)	104.0 (.6)	O(13)–*T*(6)–O(16)	110.6 (1.0)	108.9 (.6)
O(9)–*T*(3)–O(20)	104.7 (1.0)	104.2 (.6)	O(13)–*T*(6)–O(17)	109.8 (1.1)	109.4 (.6)
O(11)–*T*(3)–O(18)	117.4 (8)	117.6 (.6)	O(15)–*T*(6)–O(16)	112.1 (1.3)	113.3 (.6)
O(11)–*T*(3)–O(20)	109.0 (1.2)	107.0 (.6)	O(15)–*T*(6)–O(17)	106.6 (1.0)	105.2 (.6)
O(18)–*T*(3)–O(20)	111.7 (1.0)	112.0 (.7)	O(16)–*T*(6)–O(17)	106.1 (9)	106.0 (.6)
Mean	109.3	109.4	Mean	109.4	109.4

T(1)–O(7)–*T*(5)	131.2 (1.3)	131.9 (.8)
T(1)–O(10)–*T*(4)	133.1 (9)	134.3 (.7)
T(1)–O(20)–*T*(3)	133.0 (9)	135.3 (.8)
T(2)–O(9)–*T*(3)	133.2 (1.1)	132.2 (.7)
T(2)–O(19)–*T*(4)	132.2 (9)	133.3 (.8)
T(4)–O(17)–*T*(6)	127.5 (1.3)	128.9 (.7)
Mean	131.7	132.6

[a] Cation designators are those of the *FRO* group. Standard errors in parentheses.

stage, the inspection of the structure factors revealed that 17 strong, low-angle reflections suffered secondary extinction and were omitted in the ensuing refinement.

The site-occupancy refinement was carried out as follows. The stoichiometry as given by Kelsey and McKie (1964) for Kola aenigmatite is

$$[Na_{3.97}Ca_{0.03}]^{VIII}[Fe^{2+}_{8.06}Ti^{4+}_{2.07}Fe^{3+}_{0.47}Mg^{2+}_{0.70}Mn^{2+}_{0.59}Ca^{2+}_{0.11}]^{VI} \cdot [Si^{4+}_{11.26}Fe^{3+}_{0.53}Al^{3+}_{0.21}]^{IV}O_{40}.$$

In order to find possible distribution of Ti in octahedral sites and Fe^{3+} in tetrahedral sites, a site-occupancy refinement was carried out with the RFINE program. The relatively minor octahedral Ca^{2+}, Mn^{2+}, Mg^{2+}, and Fe^{3+} cations have been included in the Fe^{2+} estimate and

tetrahedral Al^{3+} in the "Si" estimate; each site occupancy was refined but the total was constrained to agree with the bulk chemistry.

The anisotropic refinement for cations only was also carried out in the final cycle. The final *R* index, after site and anisotropic refinement, was 7.2 percent. Anisotropic coefficients are presented in Table 5, and the thermal vibration amplitudes derived therefrom are listed in Table 6. The observed and calculated structure factors are on deposit.[2] The atomic parameters are listed in Table 1. Tables 2 and 3 give distances and angles.

Discussion of the Structure

Topology. A stereoscopic drawing (*FRO*) of the aenigmatite structure is shown in Figure 1. Figure 2 shows a clinographic projection of the atomic distribution in the triclinic cell as well as the relation between the

Table 4. Cation Site Populations in Aenigmatite

SITE \ CATION	Fe^{2+}	Ti^{4+}	SITE \ CATION	Si^{4+}	Fe^{3+}
M (1)	0.89	0.11	*T* (1)	1.00	0.00
M (2)	.87	.13	*T* (2)	1.00	.00
M (3)	.95	.05	*T* (3)	.90	.10
M (4)	.76	.24	*T* (4)	.95	.05
M (5)	.90	.10	*T* (5)	.94	.06
M (6)	1.00	.00	*T* (6)	.95	.05
M (7)	.41	.59			

triclinic cell and the monoclinic pseudo-cell. The similarity between the structures of aenigmatite and sapphirine is apparent (Figure 3). Moore (1969) describes the sapphirine structure as formed by "walls" of cation-oxygen octahedra indefinitely extended along *c* and with three or four octahedral units in the *b* direction (Figure 3a). Such "walls" are interconnected both by chains of tetrahedra running along [001] and by additional octahedra (Fig. 3b). The chains consist of pyroxene-like members, with additional "wings" of corner-sharing tetrahedra represented by two adjacent tetrahedra in the repeat unit of four tetrahedra of the chain. The layers of Figures 3a and 3b follow alternately along the *a*-axis according to the axial glide plane along *a*.

[2] To obtain a copy, order NAPS Document No. 01314 from National Auxiliary Publications Service of A.S.I.S., c/o CCM Information Corporation, 909 Third Avenue, New York, New York 10022; remitting $4.00 for microfiche or $5.60 for photocopies, in advance, payable to CCMIC-NAPS.

This arrangement is partially modified in aenigmatite, as a result of the replacement of some cation-octahedra with Na-polyhedra of a higher coordination, comparable to that of a distorted square antiprism. The octahedral "walls" are transformed into continuous layers formed by Fe- or Ti-octahedra as well as by Na-antiprisms (Figure 3c). As in sapphirine, such layers alternate in the a_m-direction with layers of Figure 3d, formed by $[Si_6O_{18}]_\infty$ chains and Fe-octahedra.

According to Figure 3, and apart from the difference in Na-coordination, the crystal structure of aenigmatite can be described as formed by unit cells of sapphirine aligned along the b_m-axis, alternately translated by $c_m/2$. Actually, since most of the atoms are nearly repeated by $c_m/2$,

TABLE 5. ANISOTROPIC TEMPERATURE FACTORS IN AENIGMATITE

SITE	β_{11}	β_{22}	β_{33}	β_{12}	β_{13}	β_{23}
M (1)	0.0018 (6)	0.0029 (6)	0.0040 (5)	0.0013 (5)	0.0013 (4)	0.0017 (5)
M (2)	.0017 (6)	.0024 (6)	.0044 (5)	.0011 (5)	.0017 (5)	.0018 (5)
M (3)	.0024 (5)	.0030 (4)	.0047 (4)	.0013 (4)	.0013 (3)	.0017 (3)
M (4)	.0029 (5)	.0032 (4)	.0047 (4)	.0017 (4)	.0018 (3)	.0020 (3)
M (5)	.0035 (5)	.0034 (4)	.0053 (4)	.0019 (4)	.0021 (3)	.0028 (3)
M (6)	.0030 (4)	.0034 (4)	.0044 (4)	.0017 (4)	.0019 (3)	.0022 (3)
M (7)	.0022 (5)	.0024 (4)	.0038 (4)	.0012 (4)	.0018 (3)	.0018 (3)
Na (1)	.0022 (11)	.0025 (10)	.0036 (9)	.0022 (9)	.0017 (8)	.0014 (8)
Na (2)	.0015 (13)	.0033 (11)	.0060 (10)	.0007 (10)	.0012 (9)	.0024 (9)
T (1)	.0010 (7)	.0011 (6)	.0021 (6)	.0003 (6)	.0008 (5)	.0007 (5)
T (2)	.0008 (7)	.0007 (6)	.0031 (6)	.0004 (6)	.0011 (5)	.0011 (5)
T (3)	.0011 (7)	.0010 (6)	.0023 (5)	.0004 (5)	.0008 (5)	.0010 (5)
T (4)	.0017 (8)	.0018 (7)	.0031 (6)	.0008 (6)	.0009 (6)	.0012 (5)
T (5)	.0019 (7)	.0024 (6)	.0024 (6)	.0016 (6)	.0015 (5)	.0015 (5)
T (6)	.0023 (7)	.0014 (6)	.0032 (6)	.0013 (6)	.0019 (5)	.0015 (5)

we can state that only the positions of the silicon atoms of the "wings" of the chains and those of Fe in the same layers as well as the positions of Ti contribute to the difference in the structure of aenigmatite with respect to that of sapphirine.

In the classification of silicates with tetrahedral frameworks suggested by Zoltai (1960), sapphirine and aenigmatite should be inserted in the new sub-type: silicates with branched single chains of tetrahedra, with a sharing coefficient of 1.5 [or 2 according to a modified definition by Coda (1969)], repeat unit 4.

Silicon tetrahedra. (*FRO*) The six crystallographically independent tetrahedral sites are also different topologically. These six tetrahedra can be

TABLE 6. MAGNITUDES AND ORIENTATION OF PRINCIPAL AXES OF THERMAL ELLIPSOIDS IN AENIGMATITE

Atom, axis	rms displacement Å(σ)	Angle, in degrees, with respect to			Atom, axis	rms displacement Å(σ)	Angle, in degrees, with respect to		
		$+a(\sigma)$	$+b(\sigma)$	$+c(\sigma)$			$+a(\sigma)$	$+b(\sigma)$	$+c(\sigma)$
$M(1)$, 1	.072 (14)	35 (18)	91 (18)	107 (12)	Na(2), 1	.064 (31)	48 (15)	78 (16)	103 (12)
2	.101 (11)	123 (18)	11 (26)	116 (25)	2	.121 (17)	128 (19)	25 (25)	124 (25)
3	.116 (8)	98 (18)	79 (26)	31 (22)	3	.147 (12)	114 (20)	68 (25)	37 (24)
$M(2)$, 1	.061 (16)	136 (17)	98 (17)	65 (8)	$T(1)$, 1	.043 (25)	57 (23)	68 (23)	113 (18)
2	.096 (12)	47 (17)	171 (17)	81 (16)	2	.077 (15)	48 (45)	138 (56)	117 (59)
3	.121 (7)	86 (12)	92 (15)	27 (9)	3	.088 (12)	60 (50)	124 (58)	37 (50)
$M(3)$, 1	.084 (8)	49 (12)	77 (13)	105 (7)	$T(2)$, 1	.027 (38)	67 (36)	58 (36)	113 (10)
2	.111 (8)	138 (13)	14 (13)	106 (17)	2	.060 (23)	24 (36)	147 (36)	93 (19)
3	.126 (5)	99 (14)	86 (17)	22 (13)	3	.102 (10)	84 (14)	96 (13)	24 (10)
$M(4)$, 1	.088 (8)	125 (17)	109 (17)	64 (8)	$T(3)$, 1	.041 (24)	109 (25)	126 (25)	64 (15)
2	.108 (8)	145 (17)	19 (17)	98 (16)	2	.076 (16)	158 (33)	37 (26)	101 (46)
3	.126 (5)	88 (14)	89 (15)	28 (8)	3	.087 (10)	100 (47)	81 (41)	29 (23)
$M(5)$, 1	.083 (8)	104 (11)	130 (10)	54 (5)	$T(4)$, 1	.068 (16)	59 (29)	66 (29)	108 (17)
2	.115 (7)	163 (12)	45 (10)	100 (13)	2	.091 (15)	149 (31)	24 (29)	100 (44)
3	.135 (5)	101 (12)	72 (10)	38 (6)	3	.103 (10)	97 (41)	88 (42)	21 (25)
$M(6)$, 1	.084 (8)	123 (10)	110 (10)	55 (8)	$T(5)$, 1	.056 (20)	148 (31)	79 (33)	53 (25)
2	.114 (7)	147 (11)	26 (21)	107 (27)	2	.080 (14)	120 (34)	19 (30)	124 (31)
3	.122 (5)	94 (28)	74 (31)	41 (16)	3	.097 (11)	79 (22)	74 (31)	55 (22)
$M(7)$, 1	.064 (10)	124 (11)	109 (12)	55 (7)	$T(6)$, 1	.053 (19)	93 (52)	141 (55)	59 (29)
2	.097 (8)	40 (12)	159 (13)	93 (15)	2	.069 (19)	25 (15)	127 (55)	116 (35)
3	.114 (6)	72 (14)	99 (15)	35 (7)	3	.109 (10)	65 (14)	100 (12)	43 (12)
Na(1), 1	.025 (81)	162 (20)	40 (22)	81 (15)					
2	.090 (17)	76 (22)	50 (22)	121 (32)					
3	.111 (14)	79 (15)	94 (23)	32 (30)					

grouped into two classes: (1) tetrahedra [$T(1)$ and $T(4)$] having one non-bridging oxygen, and (2) tetrahedra [$T(2)$, $T(3)$, $T(5)$ and $T(6)$] having two non-bridging oxygens (one of the bridges is to an octahedral Fe^{2+}). Although the non-bridging Si-O distances are generally shorter than the bridging Si-O distances, the difference is not as distinct as in other silicate structures. The angles in the silicon tetrahedra are given in Table 3. Some of the reasons for the dependence of Si-O (br) and Si-O (nbr) bond lengths on Si-O-Si angles and average electronegativity of non-tetrahedral cations are discussed by Brown and Gibbs (1970).

As can be seen from Table 2, the range of Si-O distances obtained by *CM* is 1.59 to 1.68 Å, and by *FRO* 1.593 to 1.670 Å. Although the standard deviations of the *FRO* group are smaller, the agreement is very good. The same is true, with a few exceptions, in the octahedral sites.

FIG. 1. Stereoscopic drawing of the crystal structure of aenigmatite (triclinic unit cell). The origin is at the upper left back corner of the cell with a and b parallel to the plane of the paper. $+b$ is horizontal and to the readers' right, $+a$ is sloping downward towards the readers' left and $+c$ is emerging from the plane of the paper.

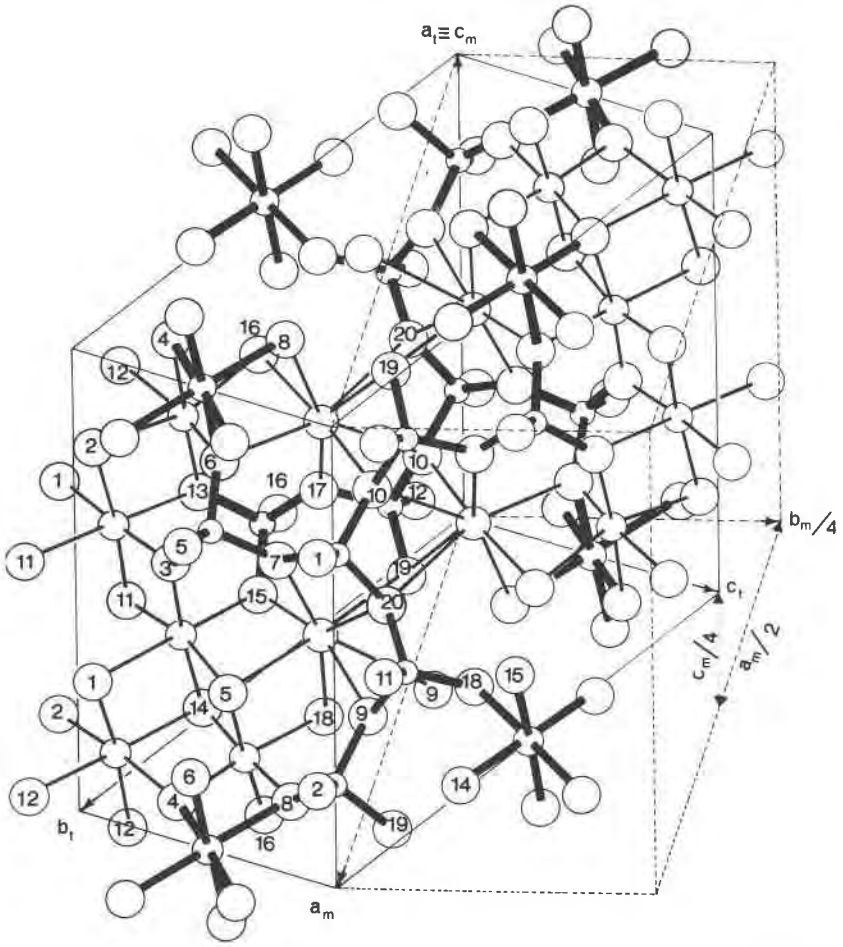

FIG. 2. Clinographic view of the atoms in the triclinic cell of aenigmatite. The bonds among atoms forming the layers of Fig. 3*d*) are drawn with heavier lines. Only the oxygen atoms are numbered; the cations can be identified from the numbers of the coordinated oxygens.

The MO_6 octahedra. (*FRO*) In Table 2 the octahedral distances are listed. All octahedra are of nearly the same size, except for the smaller Ti site. It will be seen that the Ti-O distances vary considerably: the shortest is 1.84 Å while the longest is 2.11 Å. These Ti-O distances can be divided into two categories: the longer bonds which range from 1.98 to 2.11 Å are found in the oxygen bridges (to a silicon) while the shortest two, 1.84 and 1.86 Å, do not participate in the bridge [O(4) and O(14)].

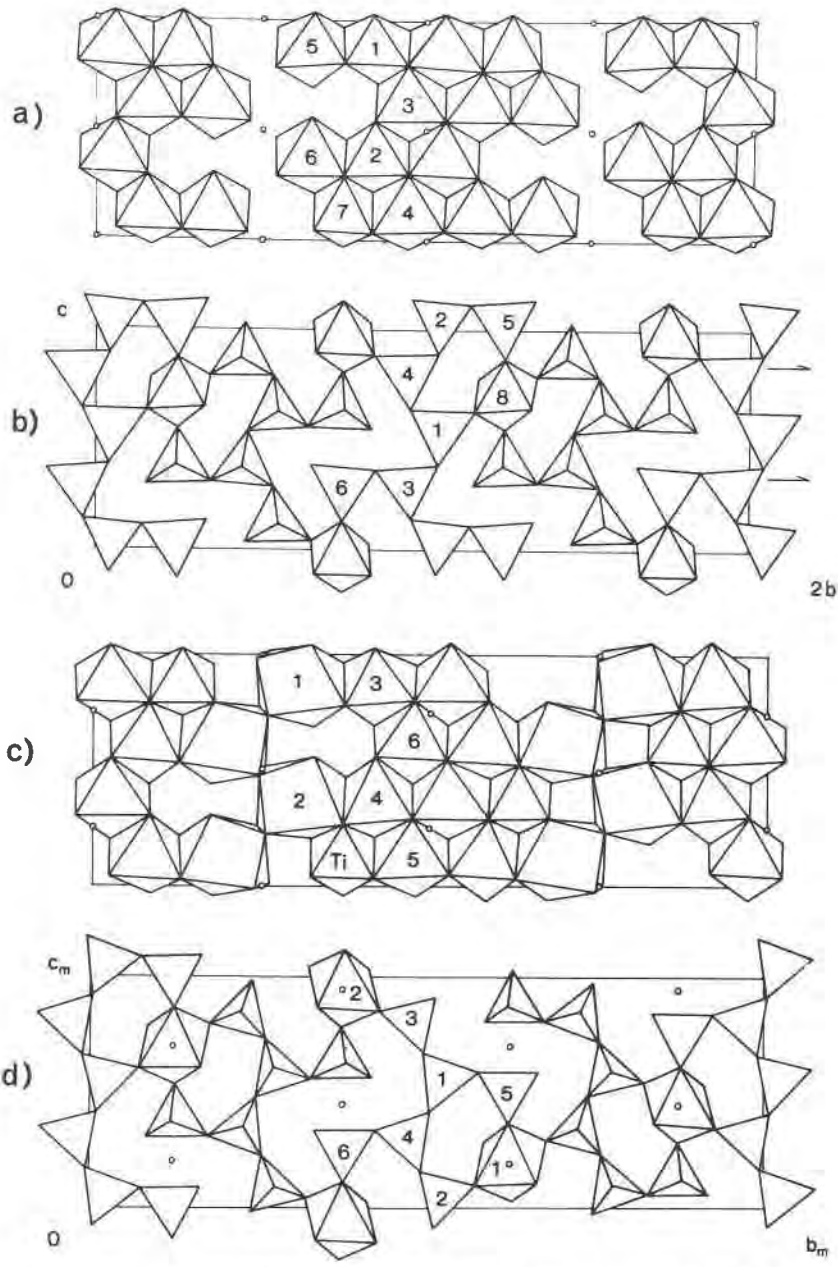

FIG. 3. *a*) Sapphirine: layer of the octahedral "walls"; *b*) sapphirine: layer of the tetrahedral chains connected by additional octahedra; *c*) aenigmatite: layer of Fe-octahedra, Ti-octahedra and Na-antiprisms; *d*) aenigmatite: layer of the $[Si_6O_{18}]_\infty$ chains connected by additional Fe-octahedra. The numbering of polyhedra in sapphirine follows Moore's paper, whereas in aenigmatite it corresponds to that of the coordinating cation.

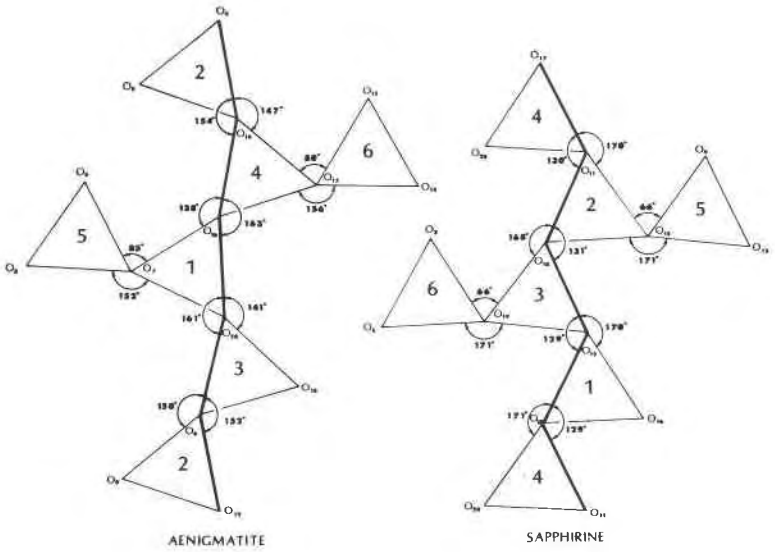

FIG. 4. A comparison of the "straightness" of the silicate chains in aenigmatite and sapphirine.

For comparison, the Ti-O distances in all three polymorphs of TiO_2 range from 1.87 to 2.04 Å (Baur, 1961). Using the effective radii of Shannon and Prewitt (1969), the distance should be $0.605+1.400=2.005$ Å. Thus the mean of 1.98 Å (CM) or 1.989 Å (*FRO*) is in excellent agreement with the experimental and theoretical values.

The octahedral angles, not reported here, range from 75° to 108° and from 160° to 180°.

Environment of the sodium cations. (*FRO*) The coordination found for Na in aenigmatite is rather common among sodium-containing silicates, such as jadeite, pectolite, glaucophane and riebeckite. The coordination is intermediate between a square antiprism and a cube. Na(1) has one long bond and Na(2) has two long bonds, as illustrated in Figure 5. The grand mean of the Na-O distances, excluding the long bonds, is 2.486 Å, comparable to 2.438 Å in riebeckite (Colville and Gibbs, 1964).

Charge balance and cation-anion bond distances. (CM) The electrostatic balance shows four "neutral" oxygens [O(1), O(2), O(11), O(12)], six "underbonded" oxygens [O(3), O(4), O(6), O(13), O(14), O(15)] (minimum sum of the strengths of the electrostatic bonds being 1.666) and ten "overbonded" oxygens (maximum sum of the bond strengths 2.25).

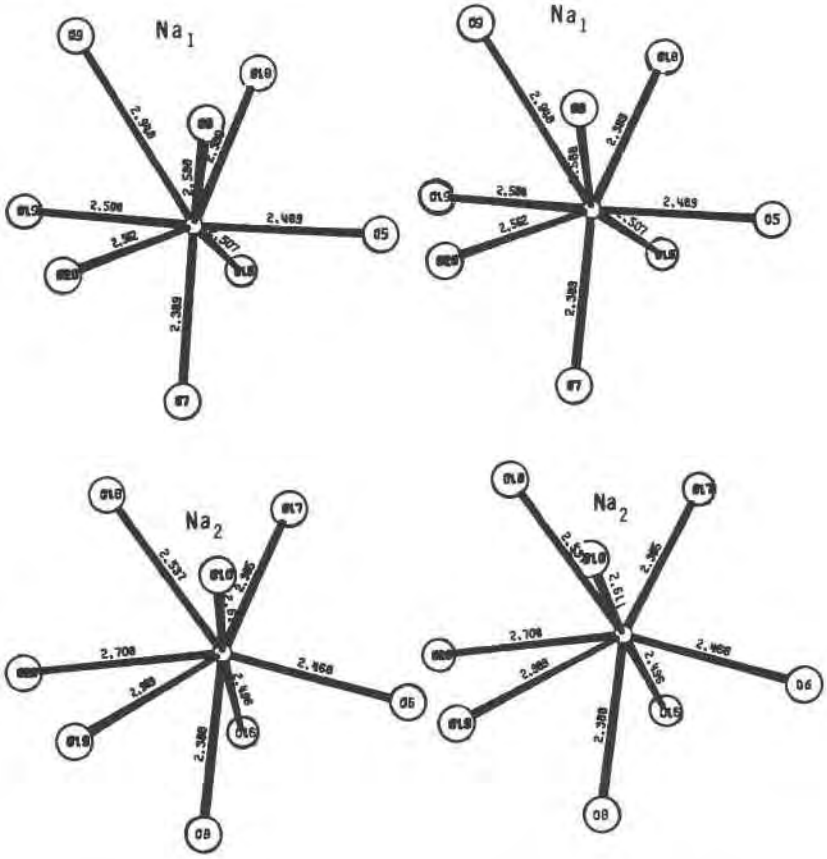

FIG. 5. Stereoscopic drawings of the coordination around Na(1) and Na(2).

The average values of the bond distances involving Fe, Ti, Na and oxygens with different degrees of saturation with respect to the positive charges arising from the coordinating cations are in Table 7. The same table shows the average Si-O distances for the oxygens "shared" between tetrahedra and for the "unshared" ones. Even if a rigorous comparison among individual distances is not possible because of the relatively high values of the standard deviations, at least the average values of Table 7 show that the Pauling-Zachariasen rules (Zachariasen, 1963), are fulfilled, particularly the increase of the distances with the increasing degree of saturation of the oxygens. The expected increase of Si–O distances when the oxygens are shared between tetrahedra, as suggested by Cruickshank (1961), is shown by the average values reported in Table 7.

TABLE 7. AVERAGE VALUES OF BOND DISTANCES[a] (Å)

Bond	Neutral oxygen atoms	Underbonded oxygen atoms	Overbonded oxygen atoms
Fe–O	2.18 [12]	2.08 [14]	2.21 [4]
Ti–O	—	1.85 [2]	2.04 [4]
Na–O	—	2.46 [2]	2.56 [14]

Bond	Shared oxygen atoms	Unshared oxygen atoms
Si–O	1.66 [12]	1.62 [12]

[a] The figures in brackets represent the number of bond distances used to obtain the average values given in the Table. These distances are calculated from the CM coordinates.

Cation site populations. (*FRO*) The procedure for obtaining the site occupancies was described under *Refinement*. Although Ti does preferentially occupy the $M(7)$ site (Table 4), it is also distributed among the other octahedral sites. However, because of the relatively high standard deviations (0.05 for Ti in M sites and 0.02 for Fe^{3+} in T sites) the values are not as accurate as they may appear.

The small amount of Fe^{3+} available for distribution concentrates in the $T(3)$ site. Prior to site refinement $B_{T(3)}$ was 0.01. However, the site refinement raised it to 0.40, in line with the other T sites. $T(3)$ is also effectively the largest of the 6 tetrahedra. It appears that $T(1)$ is also as large as $T(3)$, however, $T(1)$ has three bridging oxygen atoms, whereas $T(3)$ has only two bridging oxygens (one to Fe^{2+}), thus $T(3)$ should be smaller than $T(1)$ since the more Si-O(br) distances there are in the tetrahedra, the larger the tetrahedra. This discrepancy can be explained if we accept the result of the site refinement that most Fe^{3+} goes into the $T(3)$ site, thus enlarging the $T(3)$ tetrahedron to the size of $T(1)$ because of the larger size of Fe^{3+} compared to Si. The improvement in the electro-neutrality about the oxygens after the site refinement further substantiates this ordering scheme.

TWINNING OF AENIGMATITE

(CM) An attempt has been made in order to explain the frequent twinning in aenigmatite. Starting from the idealized triclinic structure as represented by sapphirine cells aligned along the b_m-direction and alternately translated by $c_m/2$, we can write the following structural scheme: $ABa\bar{B}Ab\bar{a}b/ABa\bar{B}Ab\bar{a}b/$ . . . Here, A(a) is a layer parallel to $(010)_m$ made up by polyhedra, which roughly are repeated at distances $b_m/2$

and $c_m/2$ [those of Fe(3), Fe(4), Fe(5), Fe(6), Na(1), Na(2), Si(1), Si(2), Si(3), Si(4)], and B(b) a parallel layer formed by polyhedra which are repeated at distances b_m and c_m [those of Fe(1), Fe(2), Ti, Si(5), Si(6)]. b is a layer equivalent to B, but translated $c_m/2$, whereas $\overline{\text{B}}$ and $\overline{\text{b}}$ are referred respectively to B and b by inversion centers. A- and a-layers are related by a_m-glide planes parallel to $(010)_m$ and passing through B-type layers: such glide planes are also real symmetry operators for the atoms of each B-type layer, but they are not for the entire structure. Both B and b layers follow in the sequence an identical A-layer, as well as $\overline{\text{B}}$ and $\overline{\text{b}}$ layers follow the a-layers.

It may be possible that, at some time during the crystallization, the sequence of pairs of B-type layers is interchanged: for instance B-layers could be replaced by b-layers and vice versa. This fact corresponds merely to a reversal of the direction of b_m and to a translation of $a_m/2$ for the entire structure. In this way, one could obtain the following scheme: ABa$\overline{\text{B}}$Aba/$\overline{\text{b}}$/Aba$\overline{\text{B}}$ABa . . . where the left side of the sequence (first individual of the twin) is symmetrical with the right one (second individual) by a $(010)_m$ a_m-glide plane passing through the /$\overline{\text{b}}$/ layer.

It is hard to imagine, as suggested by Kelsey and McKie, that aenigmatite from volcanic rocks crystallized primarily as a monoclinic polymorph, then inverted into polysynthetic twins of triclinic crystals during the cooling, since the idealized crystal structure is still triclinic. One should think that monoclinic aenigmatite has the same crystal structure as sapphirine, but its inversion to the triclinic form would imply a large migration of atoms.

It is likely that twinned aenigmatite is easily formed during the crystallization at high temperatures according to the above scheme and is "frozen" in the crystals occurring in a volcanic regime. On the contrary it is possible that, during the slow cooling of a plutonic rock, crystallization occurs in conditions of thermodynamic equilibrium so as to form untwinned triclinic crystals.

Both the crystal structures of sapphirine and aenigmatite (krinovite, rhönite, see below) represent an example of order-disorder structures (OD-structures) (Dornberger-Schiff, 1956) where the building unit is given by the layer pairs AB. The monoclinic ordered structure of sapphirine (ABa$\overline{\text{B}}$) is apparently more stable when large cations (Na, Ca) are missing, whereas the ordered triclinic structure of aenigmatite (krinovite, rhönite) (ABa$\overline{\text{B}}$Ab$\overline{\text{a}}$) is formed in presence of Na or Ca. In any case, because of the easy replacement of the AB pair for the Ab pair (or a$\overline{\text{B}}$ for a$\overline{\text{b}}$) in the way above described, a large range of disordered structures can be possible (McKie, 1963; Merlino, private communication).

Related Structures

(*FRO*) The similarity of the structures of aenigmatite and sapphirine has been mentioned. In fact, the knowledge of the sapphirine structure aided in unravelling the Patterson syntheses. However, differences are also evident. Figure 4 shows the "straightness" of the $[Si_6O_{18}]_\infty$ chains in both structures. As can be seen, the O-O-O angles are such that the aenigmatite chains would be more nearly similar to those of pyroxene. The dissimilarity is also borne out by the fact that the oxygens in sapphirine are close-packed (16.39 Å^3 per oxygen atom), spinel-like, whereas a volume of 18.6 Å^3 per oxygen atom in aenigmatite is too loose to approximate close-packing; in fact, the volume per oxygen atom is more in line with 17.8 Å^3 in aegirine and 18.7 Å^3 in riebeckite (Kelsey and McKie, 1964).

Another related structure is that of rhönite (Cameron, Carman and Butler, 1970; Walenta, 1969). The composition, morphology and crystal cell parameters of rhönite are suggestive of the similarity between the two minerals. Furthermore, rhönite has the same sapphirine-like monoclinic pseudo-cell and exhibits polysynthetic twinning parallel to (010) of the pseudo-cell. The idealized formula for rhönite is $Ca_4(Mg, Fe^{2+})_8 \cdot Fe_2^{3+}Ti_2Al_6Si_6O_{40}$, indicating substitutions of Ca for Na, Fe^{3+} and some Mg for Fe^{2+}, and Al for Si. The last substitution is analogous to the sapphirine composition. The second substitution is quite interesting: if we assume that rhönite is structurally related to aenigmatite, then Fe^{3+} will occupy an octahedral site. Is this octahedral Fe^{3+} ordered . . . is it in a high- or low-spin state? These and other aspects of crystal chemistry are of considerable interest and must await complete structural analysis of the mineral. Thus we are in the process of studying rhönite.

As pointed out by Merlino (1970b), also krinovite, $NaMg_2CrSi_3O_{10}$, has a crystal structure related to that of aenigmatite. Merlino suggests that Cr could replace iron in *M*1, *M*2 and *M*8 and Mg could replace iron in the remaining octahedra.

Acknowledgments

The FRO group wishes to thank Professor McKie, Cambridge University, for supplying the untwinned crystals of aenigmatite and for his interest in the structure, to Dr. Finger of the Geophysical Laboratory, who advised us in the use of his RFINE program, and to the Southern Illinois University Computing Center for generous allocations of computer time.

This work was supported by an NSF Grant GA 19688 (*FRO* group).

References

Baur, W. H. (1961) Über die Verfeinerung der Kristallstrukturbestimmeng einiger Vertreter des Rutiltyps III. Zur Gittertheorie des Rutiltyps. *Acta Crystallogr.* **14**, 209–213.

BEDNOWITZ, A. L. (1970) SORTE—A program to aid in the implementation of the symbolic addition method for the direct determination of centrosymmetric crystal structures. In F. R. Ahmed, (ed.), *Crystallographic Computing*, Munksgaard, Copenhagen, Denmark, p. 58–62.

BROWN, G. E., AND G. V. GIBBS (1970) Stereochemistry and ordering in the tetrahedral portion of silicates. *Amer. Mineral.* **55,** 1587–1607.

CAMERON, K. L., M. F. CARMAN, AND J. C. BUTLER (1970) Rhönite from Big Bend National Park, Texas, *Amer. Mineral.* **55,** 864–874.

CODA, A. (1969) La classificazione di alcuni silicati secondo Zoltai. *Rend. Soc. Ital. Mineral. Petrologia* **25,** 195–226.

COLVILLE, A., AND G. V. GIBBS (1964) Refinement of the crystal structure of riebeckite [abstr.]. *Geol. Soc. Amer. Spec. Pap.* **82,** 31.

CROMER, D. T., AND J. B. MANN (1968) X-ray scattering factors computed from numerical Hartree-Fock wave functions. *Acta Crystallogr.* **A24,** 321–324.

CRUICKSHANK, D. W. J. (1961) The role of 3d-orbitals in π-bonds between (a) silicon, phosphorus, sulphur or chlorine and (b) oxygen or nitrogen. *J. Chem. Soc.* **1961,** 5486–5504.

DORNBERGER-SCHIFF, K. (1956) On order-disorder structures (OD-structures). *Acta Crystallogr.* **9,** 593–601.

FINGER, L. W. (1969) The crystal structure and cation distribution of a grunerite. *Mineral. Soc. Amer. Spec. Pap.* **2,** 95–100.

HANSON, H. P., F. HERMAN, J. D. LEA, AND S. SKILLMAN (1964) HFS atomic scattering factors. *Acta Crystallogr.*, **17,** 1040–1044.

KELSEY, C. H., AND D. MCKIE (1964) The unit-cell of aenigmatite. *Mineral. Mag.* **33,** 986–1001.

MCKIE, D. (1963) Order-disorder in sapphirine. *Mineral. Mag.* **33,** 635–645.

MERLINO, S. (1970a) Crystal structure of aenigmatite. *Chem. Comm.* **20,** 1288–1289.

——— (1970b) X-ray crystallography of krinovite. *Contrib. Mineral. Petrology,* (in press).

MOORE, P. B. (1969) The crystal structure of sapphirine. *Amer. Mineral.* **54,** 31–49.

SHANNON, R. D., AND C. T. PREWITT (1969) Effective ionic radii in oxides and fluorides. *Acta Crystallogr.* **B25,** 925–946.

WALENTA, K. (1969) Zur Kristallographie des Rhönits., *Z. Kristallogr.* **130,** 214–230.

ZACHARIASEN, W. H. (1963) The crystal structure of monoclinic metaboric acid. *Acta Crystallogr.* **16,** 385–389.

ZOLTAI, T. (1960) Classification of silicates and other minerals with tetrahedral structures. *Amer. Mineral.* **45,** 960–973.

Manuscript received, August 7, 1970; accepted for publication, December 29, 1970.